

# Incoherent-Light Temporal Imaging Based on a Temporal Pinspeck

Bo Li, *Student Member, IEEE*, Shuqin Lou, *Member, IEEE*, and José Azaña, *Member, IEEE*

**Abstract**—Incoherent-light temporal imaging using a temporal pinhole camera has been recently proposed and demonstrated as a way to improve the key limitations of coherent temporal imaging systems. However, the energy efficiency of incoherent-light temporal imaging is greatly limited by the narrow temporal pinhole, which filters out most of the incoming light along the time domain. In this letter, we propose and experimentally demonstrate a novel incoherent-light temporal imaging scheme based on a temporal pinspeck, which is a time-domain equivalent of a spatial pinspeck. In contrast to a temporal pinhole, the temporal pinspeck keeps most of the incoming light, greatly improving the system’s energy efficiency. In addition, the performance specifications of temporal-pinspeck-based systems, such as temporal apertures and resolutions, are subject to similar design tradeoffs as their temporal-pinhole-based counterparts.

**Index Terms**—Incoherent-light signal processing, temporal imaging, time-to-frequency mapping, frequency-to-time mapping, temporal pinspeck.

## I. INTRODUCTION

TEMPORAL imaging [1], [2], time-to-frequency mapping [3] and frequency-to-time mapping [4] have been extensively used for generation [1], [4], measurement [1], [3] and processing [1], [2] of radio-frequency (RF) signals and optical waveforms. Conventional temporal imaging, time-to-frequency mapping and frequency-to-time mapping are based on coherent optics. Generally, the performance of these systems essentially depends on the light source bandwidth (performance is improved as the optical bandwidth is increased); however, coherent light sources capable of providing large frequency bandwidths are typically complex and costly.

Compared to coherent light sources, incoherent optical sources are more practical and closer to those found in

Manuscript received September 11, 2014; revised November 4, 2014; accepted November 14, 2014. Date of publication November 20, 2014; date of current version January 21, 2015. This work was supported in part by the Natural Science and Engineering Research Council of Canada and in part by the China Scholarship Council for the Graduate Fellowships.

B. Li is with the School of Electronic and Information Engineering, Beijing Jiaotong University, Beijing 100044, China, and also with the Institut National de la Recherche Scientifique-Energie, Matériaux et Télécommunications, Montréal, QC H5A 1K6, Canada (e-mail: liboresearch@gmail.com).

S. Lou is with the School of Electronic and Information Engineering, Beijing Jiaotong University, Beijing 100044, China (e-mail: shglou@bjtu.edu.cn).

J. Azaña is with the Institut National de la Recherche Scientifique-Energie, Matériaux et Télécommunications, Montréal, QC H5A 1K6, Canada (e-mail: azana@emt.inrs.ca).

Color versions of one or more of the figures in this letter are available online at <http://ieeexplore.ieee.org>.

Digital Object Identifier 10.1109/LPT.2014.2372752

nature. Besides that, it is easier for an incoherent light source to provide a large frequency bandwidth [1]–[4]. Therefore, incoherent-light temporal imaging, time-to-frequency mapping and frequency-to-time mapping systems have been proposed and demonstrated to improve these limitations [5]–[7]. These incoherent systems typically involve the combination of dispersion and temporal pinholes. A temporal pinhole refers to short temporal gating of the incoming light [7], [8]. The concept of a temporal pinhole is key for realization of these incoherent systems. However, similarly to systems based on spatial pinholes, there is a limiting trade-off between the resolution and energy efficiency in these systems, i.e., to have a good resolution, the duration of the temporal pinhole should be sufficiently short, which necessarily leads to a low energy efficiency because most of the incoming light is filtered out along the time domain by the narrow temporal pinhole [7].

Here we propose and experimentally demonstrate the concept of a temporal pinspeck with the aim of improving the energy efficiency of these incoherent-light systems. A temporal pinspeck is the temporal counterpart of a spatial pinspeck [9]–[11], and can be interpreted as a ‘dark’ temporal pinhole (inverted temporal pinhole on a bright background). In particular, a temporal pinhole filters out all the incoming light beyond the narrow central area, while a temporal pinspeck keeps (filters in) most of the incoming light except that in the narrow central area, as shown in the illustrations Fig. 1(b) and Fig. 1(c). Thus, the energy efficiency of a temporal-pinspeck-based system is greatly superior to that of a temporal-pinhole-based system whereas the temporal resolutions for these two different systems are similar. In this letter, we numerically demonstrate the possibility of implementing incoherent-light temporal imaging, time-to-frequency mapping and frequency-to-time mapping using a temporal pinspeck process. Proof-of-concept experiments for incoherent-light temporal imaging and time-to-frequency mapping are also provided.

## II. PRINCIPLE OF OPERATION

An illustration of the proposed scheme for incoherent-light temporal imaging based on a temporal pinspeck is shown in Fig. 1(a). In brief, light from a broadband, temporally incoherent light source is intensity modulated by the input waveform to be processed. The modulated light is sent through the input dispersion, which is a medium that provides a group-delay dispersion of  $\Phi_{In}$  (slope of group-delay as a function

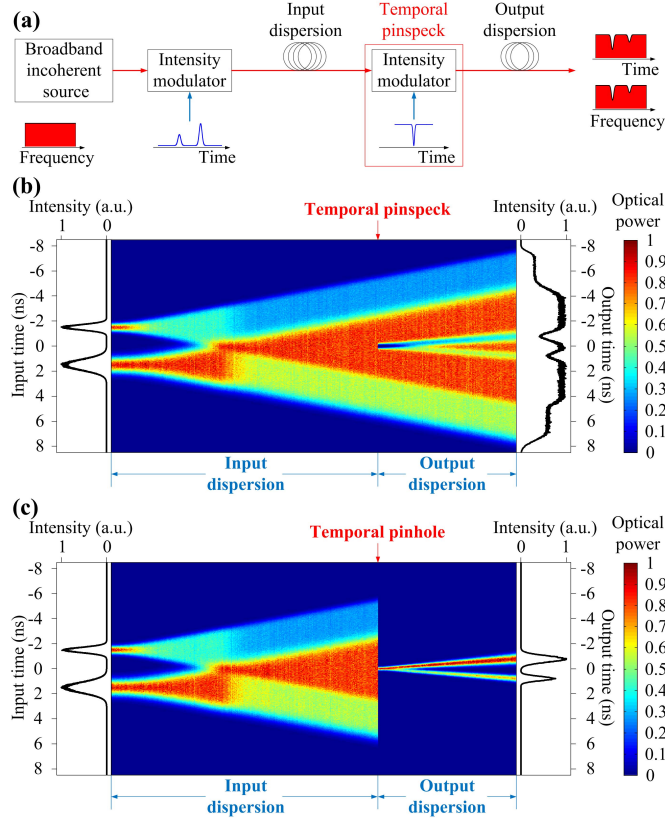


Fig. 1. Incoherent-light temporal imaging schemes. (a) Diagram of an incoherent-light temporal imaging system based on a temporal pinspeck. (b) The evolution of the signal for the incoherent-light temporal imaging process based on a temporal pinspeck. (c) The evolution of the signal for the incoherent-light temporal imaging process based on a temporal pinhole. In examples (b) and (c), the input signals are both two Gaussian-like pulses with different time widths.

of angular frequency) over the entire bandwidth of the light source. The following step involves sending the light through a temporal intensity modulation process, implementing the temporal pinspeck. Finally, the output of the temporal pinspeck is dispersed through the output dispersion, which introduces a group-delay dispersion of  $\ddot{\Phi}_{Out}$ . The temporal optical intensity profile in average at the system output is a scaled (magnified or compressed) ‘dark’ image of the input temporal intensity waveform. Similarly to a temporal pinhole system [7], the system magnification factor is given by the output to input dispersions ratio,  $M = -\ddot{\Phi}_{Out}/\ddot{\Phi}_{In}$ .

Additionally, the averaged spectrum at the system output is also a scaled dark image of the input temporal intensity waveform. This incoherent-light time-to-frequency mapping process is implemented by the input dispersion and temporal pinspeck process (no need for the output dispersion in this case), where the time-to-frequency mapping factor is dictated by the input dispersion. Indeed, as for the temporal pinhole case [7], the described incoherent-light temporal imaging process can be interpreted as consisting of two main steps, namely time-to-frequency mapping (implemented by the input dispersion + pinspeck) and frequency-to-mapping (induced by the output dispersion), respectively.

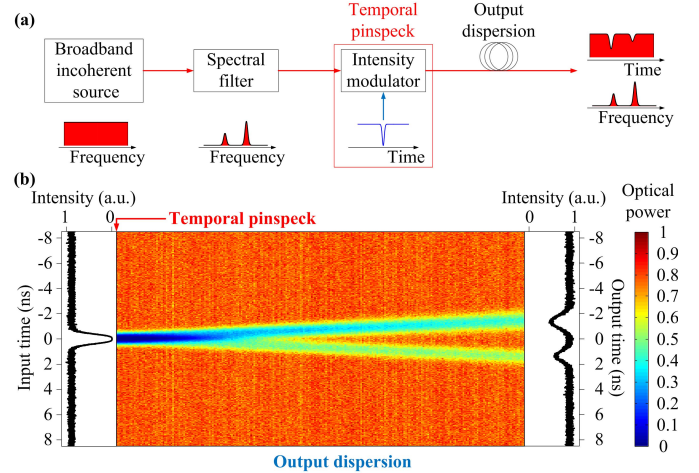


Fig. 2. Incoherent-light frequency-to-time mapping system. (a) Diagram of incoherent-light frequency-to-time mapping system based on temporal pinspeck. (b) The evolution of the signal along the output dispersive medium in (a). The input signal consists of two Gaussian-like pulses with different time widths.

The temporal pinspeck can be also used for building up an incoherent-light frequency-to-time mapping system, as shown in Fig. 2(a), using a similar configuration to that of the system based on a temporal pinhole [5]–[7]. The spectrum with the profile to be processed is obtained by spectrally filtering the incoherent light source. The filtered light is then sent through the temporal pinspeck and the following output dispersion. At the system output, the temporal optical intensity profile in average is a scaled dark image of the input spectrum. The evolution of the light along the pinspeck and output dispersive medium is illustrated in Fig. 2(b). Two dark pulses are generated as the signal propagates through the output dispersive medium.

In general, the configurations of the proposed pinspeck-based systems for temporal imaging, time-to-frequency mapping and frequency-to-time mapping are identical to their temporal-pinhole-based counterparts, except for the difference in the used temporal modulation waveform [5]–[7]. Thus, the performance specifications of the pinspeck-based systems, particularly temporal aperture and temporal/spectral resolutions, follow a similar set of design equations as those previously derived for the pinhole-based schemes, depending on the light source bandwidth, temporal pinhole duration and values of the input and output dispersions [7]. For instance, the input temporal aperture for a pinspeck-based temporal imaging system is given by  $T_A = \pi |\ddot{\Phi}_{In}| \Delta f_{Source}$ . This value is half of the input temporal aperture for a pinhole-based system [7], which is due to that the output signal can be distinguished only if they are within the central flat area, as shown in Fig. 1(b). Additionally, the optimal duration [intensity full width at half maximum (FWHM)] of a ‘dark’ Gaussian-like pinspeck is  $\Delta T_{P,opt} \approx 2\sqrt{\ln 2} |\ddot{\Phi}_{In} \ddot{\Phi}_{Out}| / (\ddot{\Phi}_{In} + \ddot{\Phi}_{Out})$ , corresponding to an input resolution of  $\delta T_{In} = |(\ddot{\Phi}_{In} + \ddot{\Phi}_{Out})/\ddot{\Phi}_{Out}| \Delta T_P$ , assuming that the pinspeck has a ‘dark’ Gaussian profile. These two values are the same as those for a pinhole-based system [7].

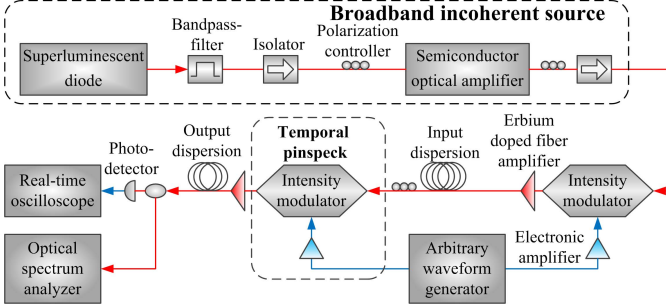


Fig. 3. Experimental setup of the incoherent-light temporal imaging system.

### III. NUMERICAL AND EXPERIMENTAL RESULTS

Fig. 3 illustrates the experimental setup used for proof-of-concept demonstration of the proposed incoherent-light temporal imaging system. The system is configured for temporal compression. Broadband incoherent light with a nearly uniform spectrum is generated by filtering a superluminescent diode at first, and then amplified by a semiconductor optical amplifier [7]. The broadband incoherent light is sent through a 40-GHz electro-optic intensity modulator, which is driven by the RF temporal waveform to be processed. The RF temporal waveform is generated by a 12-Gsamples/s electronic arbitrary waveform generator and then amplified by a 12-GHz electronic amplifier. The modulated light, which has the same profile as the RF temporal waveform, is defined as the input signal of the temporal imaging system. The input signal is sent through the input dispersive line, which introduces a dispersion of  $-1326 \text{ ps/nm}$ , and the temporal pinspeck, which is realized by another 40-GHz electro-optic intensity modulator driven by an electronic pulse waveform generated by the same arbitrary waveform generator and subsequently amplified by a 12.5-GHz electronic amplifier. After the temporal pinspeck, the light is sent through the output dispersive line, which introduces a dispersion of  $-692 \text{ ps/nm}$  and as such the magnification factor is given by  $M = -(-692)/(-1326) = -1/1.92$ . Subsequently the system temporal output is detected by a 45-GHz photo-detector and measured by a 28-GHz real-time oscilloscope, whereas the system output spectrum is measured by an optical spectrum analyzer.

The numerical (red lines) and experimental (black lines) results for incoherent-light temporal imaging are shown in Fig. 4. We did two experiments using two different input signals, which are shown in Fig. 4(b) and Fig. 4(g), respectively. The bandwidth of the incoherent light source used for the two experiments [Fig. 4(a) and Fig. 4(f)] is  $\sim 6 \text{ nm}$ . Fig. 4(c) and Fig. 4(h) show the outputs of the temporal pinspeck for these two experiments, respectively, where the intensity FWHM of the temporal pinspeck is  $\sim 146 \text{ ps}$ . Finally, the measured temporal waveforms at the system output are shown in Fig. 4(d) and Fig. 4(i), respectively. In Fig. 4(d), the output time widths for simulation and experiment are respectively  $\Delta T_{1s} = 270 \text{ ps}$  and  $\Delta T_{1e} = 290 \text{ ps}$ , which are slightly higher than the theoretical expectation of  $\Delta T_{1t} = 497|M| \text{ ps} \approx 259 \text{ ps}$ ; In Fig. 4(i), the time separations between the output two ‘dark’ pulses for simulation and experiment are both about  $\Delta T_{2e} = 0.835 \text{ ns}$ , which is exactly

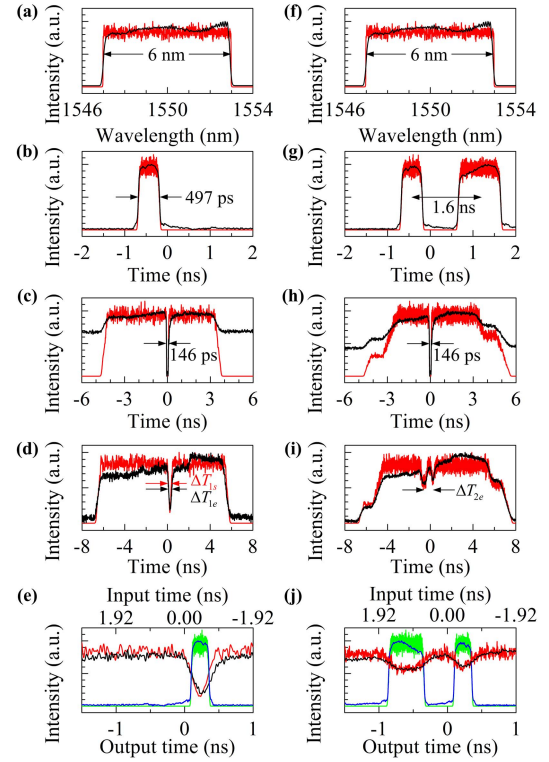


Fig. 4. Numerical (red) and experimental (black) demonstration of incoherent-light temporal imaging. Two experiments with different input signals are shown in (a)-(e) and (f)-(j), respectively. (a), (f) Spectra of incoherent light sources. (b), (g) Temporal waveforms of input signals. (c), (h) Temporal outputs of temporal pinspecks. (d), (i) Temporal outputs of the system. (e), (j) Temporal outputs versus scaled input signals obtained in simulation (green) and experiment (blue), where the scaling is  $M = -1/1.92$ . All the profiles are averaged for 256 times.

the same as the theoretical expectation of  $\Delta T_{2t} = 1.6|M| \text{ ns} \approx 0.835 \text{ ns}$ . As predicted, the measured outputs are temporally compressed dark images of the corresponding input temporal signals [see Fig. 4(e) and Fig. 4(j)].

For completeness, Fig. 5 shows results on incoherent-light time-to-frequency mapping using the same experimental setup (Fig. 3) but with a broader light source bandwidth ( $\sim 7.7 \text{ nm}$ ), see simulated and measured spectra shown in Fig. 5(a) and (f). We again did two experiments to prove our concept. The input signals for the two experiments are shown in Fig. 5(b) and Fig. 5(g), respectively. The temporal outputs of the temporal pinspeck for these two experiments are shown in Fig. 5(c) and Fig. 5(h), respectively, where the intensity FWHM of the temporal pinspeck is  $\sim 608 \text{ ps}$ . Finally, the measured spectra at the system output are shown in Fig. 5(d) and Fig. 5(i), respectively. In Fig. 5(d), the output spectral widths for simulation and experiment are  $\Delta \lambda_{1s} = \Delta \lambda_{1e} = 0.49 \text{ nm}$ , which are slightly higher than the theoretical expectation of  $\Delta \lambda_{1t} = -(497 \text{ ps})/(1326 \text{ ps/nm}) \approx 0.37 \text{ nm}$ ; In Fig. 5(i), the wavelength separations between the output two ‘dark’ pulses for simulation and experiment are both about  $\Delta \lambda_{2e} = 1.18 \text{ nm}$ , which is similar to the theoretical expectation of  $\Delta \lambda_{2t} = -(1.6 \text{ ns})/(1326 \text{ ps/nm}) \approx 1.2 \text{ nm}$ . As predicted, time-to-frequency mapping has been achieved at the output of the temporal pinspeck, as shown in Fig. 5(e) and Fig. 5(j).

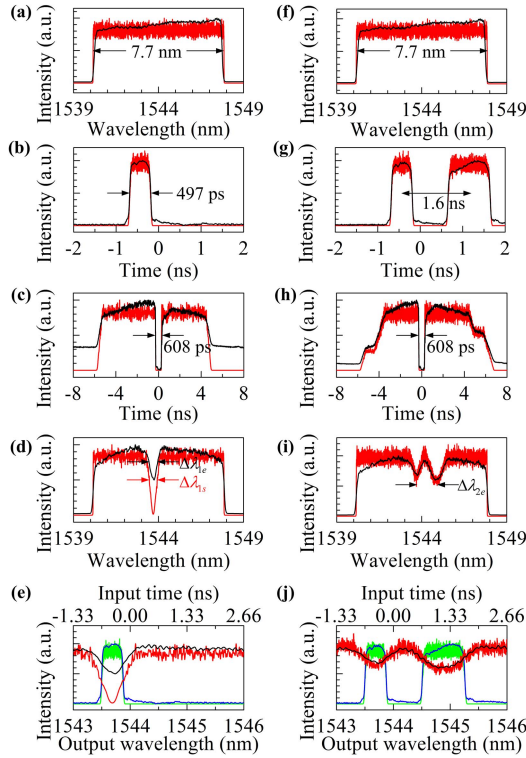


Fig. 5. Numerical (red) and experimental (black) demonstration of incoherent-light time-to-frequency mapping. Two experiments with different input signals are shown in (a)-(e) and (f)-(j), respectively. (a), (f) Spectra of incoherent light sources. (b), (g) Temporal waveforms of input signals. (c), (h) Temporal outputs of temporal pinspecks. (d), (i) Spectral outputs of temporal pinspecks. (e), (j) Spectral outputs versus scaled input signals obtained in simulation (green) and experiment (blue), where the scaling is  $-1326 \text{ ps/nm}$ . All the profiles are averaged for 256 times.

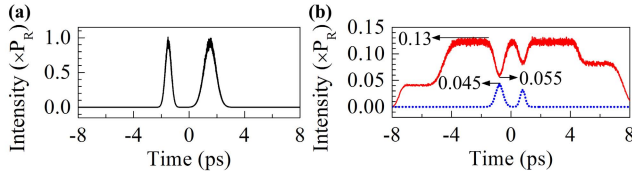


Fig. 6. Comparison between the pinhole and pinspeck cases for the temporal imaging. (a) Input optical waveform for two cases, where the peak power of the input waveform is given by  $P_R$ . (b) Output temporal waveforms for pinhole (dotted blue) and pinspeck (solid red) cases.

To illustrate the predicted energy efficiency improvement, we show a numerical comparison between the pinhole and pinspeck cases for the temporal imaging experiments shown in Fig. 6. The same input optical waveform is used in these two cases, as shown in Fig. 6(a). The corresponding output temporal waveforms are shown in Fig. 6(b). From Fig. 6, one can easily infer the pinspeck exhibits a much higher energy efficiency than the pinhole. In particular, the output energy for the pinspeck case is  $\sim 36$  times higher than that for the pinhole case.

#### IV. DISCUSSION AND CONCLUSION

As discussed, the energy efficiency of the temporal pinspeck-based systems is significantly higher than those

based on a temporal pinhole, while the system performance specifications, such as aperture, resolution and scaling factor, depend on the system parameters – light source bandwidth, pinspeck duration and dispersion values – following the same set of equations, except that the aperture is half of that for a pinhole-based temporal imaging system. In addition, the system could be also upgraded for single-shot temporal imaging by using a suitable broadband discrete-spectrum (multi-wavelength) laser source instead of the continuous-spectrum incoherent-light source reported in this letter [7]. Nonetheless, a critical shortcoming of the proposed systems is that the output waveform exhibits a worse signal-to-noise ratio (SNR) when employing a pinspeck. We attribute this degradation to the fact that the temporal pinspeck allows more light, including a larger noise contribution, to pass through the system. It should be noted that the SNR degradation is more significant as the input signal duration is increased, i.e. for more complex input waveforms. Consequently, we believe the pinspeck concept may be particularly useful for processing relatively simple waveforms, i.e., with relatively low time-bandwidth products (TBP); however, the pinspeck performance may be significantly more limited for processing more complex, high-TBP waveforms.

In summary, we have theoretically and experimentally demonstrated incoherent-light temporal imaging, time-to-frequency mapping and frequency-to-time mapping of optical waveforms using the time-domain equivalent of a spatial pinspeck camera. The demonstrated concept should enrich the family of incoherent-light signal processing tools.

#### REFERENCES

- [1] B. Kolner, "Space-time duality and the theory of temporal imaging," *IEEE J. Quantum Electron.*, vol. 30, no. 8, pp. 1951–1936, Aug. 1994.
- [2] Y. Han and B. Jalali, "Photonic time-stretched analog-to-digital converter: Fundamental concepts and practical considerations," *J. Lightw. Technol.*, vol. 21, no. 12, pp. 3085–3103, Dec. 2003.
- [3] M. A. Foster, R. Salem, D. F. Geraghty, A. C. Turner-Foster, M. Lipson, and A. L. Gaeta, "Silicon-chip-based ultrafast optical oscilloscope," *Nature*, vol. 456, pp. 81–84, Nov. 2008.
- [4] J. Van Howe and C. Xu, "Ultrafast optical signal processing based upon space-time dualities," *J. Lightw. Technol.*, vol. 24, no. 7, pp. 2649–2662, Jul. 2006.
- [5] V. Torres-Company, J. Lancis, and P. Andrés, "Incoherent frequency-to-time mapping: Application to incoherent pulse shaping," *J. Opt. Soc. Amer. A*, vol. 24, no. 3, pp. 888–894, Mar. 2007.
- [6] C. Dorner, "Statistical analysis of incoherent pulse shaping," *Opt. Exp.*, vol. 17, no. 5, pp. 3341–3352, Mar. 2009.
- [7] B. Li and J. Azaña, "Incoherent-light temporal stretching of high-speed intensity waveforms," *Opt. Lett.*, vol. 39, no. 14, pp. 4243–4246, Jul. 2014.
- [8] B. H. Kolner, "The pinhole time camera," *J. Opt. Soc. Amer. A*, vol. 14, no. 12, pp. 3349–3357, Dec. 1997.
- [9] A. T. Young, "Television photometry: The Mariner 9 experience," *Icarus*, vol. 21, no. 3, pp. 262–282, 1974.
- [10] J. Walker, "The pleasure of the pinhole camera and its relative the pinspeck camera," *Sci. Amer.*, vol. 245, no. 11, pp. 192–200, 1981.
- [11] M. Young, "The pinhole camera: Imaging without lenses or mirrors," *Phys. Teacher*, vol. 27, no. 9, pp. 648–655, Dec. 1989.